

Root Cause Analysis of Low Throughput Situations Using Boosting Algorithms and the TreeShap Analysis

M. Cilínio¹ and D. Duarte²

¹Instituto Superior Técnico

²CELFINET,

Consultoria em Telecomunicações, Lda.

Lisbon, Portugal

madalena.ramos@tecnico.ulisboa.pt,

david.duarte@celfinet.com

P. Vieira^{3,4}

³Instituto Superior de Engenharia Lisboa

Lisbon, Portugal

pedro.vieira@isel.pt

M. P. Queluz^{1,4} and A. Rodrigues^{1,4}

⁴Instituto de Telecomunicações,

Lisbon, Portugal

[ar, paula.queluz]@lx.it.pt

Abstract—Detecting and diagnosing the root cause of failures in mobile networks is an increasingly demanding and time-consuming task, given its technological growing complexity. This paper focuses on predicting and diagnosing low User Downlink (DL) Average Throughput situations, using supervised learning and the Tree Shapley Additive Explanations (SHAP) method. To fulfill this objective, Boosting classification models are used to predict a failure/non-failure binary label. The influence of each counter on the overall model's predictive performance is performed based on the TreeSHAP method. From the implementation of this technique, it is possible to identify the main causes of low throughput, based on the analysis of the most critical counters in fault detection. Furthermore, from the identification of these counters, it is possible to define a system for diagnosing the most probable throughput degradation cause. The described methodology allowed not only to identify and quantify low throughput situations in a live network due to the occurrence of misadjusted configuration parameters, radio problems and network capacity problems, but also to outline a process for solving them.

Index Terms—Mobile Networks, KPIs, PM Indicators, Supervised Learning, Boosting Classification Models, TreeSHAP

I. INTRODUCTION

The exponential complexity growth of mobile networks and its technology has brought challenges in performing the Root Cause Analysis (RCA) of network performance degradation resorting only to human input. For this reason, Mobile Network Operators (MNOs) have turned their attention to automating this analysis, by introducing Self-Healing functions divided into three primary areas: Detection, Diagnosis and Compensation [1]. These functions are based on correlation and statistical analysis of alarms, mobile traces, configuration parameters, network counters and Key Performance Indicators (KPIs), collected from faulty cells [2]. Thus, Machine Learning (ML) techniques have emerged as a powerful tool to develop Self-Healing networks, due to their ability to learn from the available data to effectively reproduce the decisions made by human experts.

Consequently, some research has already been conducted to design systems capable of performing the RCA of Integrity KPIs failures using ML techniques. Namely, in [3] the authors propose a Deep Neural Network (DNN) architecture to perform the RCA of poor throughput in mobile networks. Furthermore, the importance of each feature was computed by applying the Local Interpretable Model-Agnostic Explanations (LIME) method.

Thus, the main objective of this work is to contribute to the detection and diagnosis of the network Integrity KPIs failures, through the identification of the Performance Management (PM) counters with the greatest influence on low User DL Average Throughput predictions. While "Boosting" classification models are used to predict failures, the identification of the most important PM counters to anticipate failures is performed using the SHAP method. In this context, the main contributions of this paper can be summarized as follows: i) Implementation of a low User DL Average Throughput diagnostic system based on PM counters measured from a real mobile network and ii) Introduction of a feature filtering method that speeds up the low throughput diagnosis process by reducing the total number of influential PM counters to be analysed by network engineers.

This work is organized as follows: Section II summarizes the proposed research methodology; Section III presents the obtained results for the failure prediction models and the respective SHAP method implementation; Section IV analyzes the output of the SHAP method in order to identify the most critical PM counters used in the elaboration of a failure RCA flowchart. Ultimately, Section V presents the final conclusions and research guidelines for future work.

II. METHODOLOGY

The PM counters used in the elaboration of this work were obtained from a real MNO, having been collected from a live Long Term Evolution (LTE) network. The data extraction was performed with an hourly granularity, over a period of 28

days, from 51 local cells, divided by 19 sites, supporting the LTE800, LTE900, LTE1800 and LTE2100 (MHz) frequency bands. The resulting dataset comprised a total of 337 PM counters. Through the combination of the collected PM counters, the User DL Average Throughput (Mbps) KPI was calculated using the following equation:

$$UserDLAvgThp = \frac{UserDLRmvLastTTITrafficVolume}{UserDLRmvLastTTITransferTime} \quad (1)$$

given by the ratio between the total DL traffic volume and the DL data transmission duration, excluding the data scheduled in the last Transmission Time Interval (TTI) before the DL buffer is empty [4].

The proposed methodology considers the following steps, described in the next sub-sections.

A. Data Pre-Processing and Feature Selection

Since the data was collected from a live network, being subject to extraction failures, it was necessary to perform data pre-processing and some feature selection processes first. These processes were implemented considering the following steps:

- Removal of PM counters with high percentage of missing values;
- Removal of rows with missing values;
- Elimination of data artifacts;
- Elimination of PM counters with null variance;
- Elimination of one of two PM counters if the mutual Pearson correlation is equal to one.

B. Labelling

The failures detection techniques using classification problems imply the existence of a discrete dependent variable. Thereby, a binary faulty/not faulty label was defined, by applying degradation threshold values provided by the MNO. Therefore, *label 1* was assigned to failures, while *label 0* was assigned to not faulty samples. After defining the dependent discrete variable for the User DL Average Throughput KPI, the counters used in its calculation, as well as counters redundant to these, were eliminated from the feature set to avoid the occurrence of overfitted models.

C. Machine Learning Techniques

Although ML classification algorithms are a powerful tool in detecting network failures, there are still challenges related to their implementation that need to be considered [5]:

- **Cost Insensitivity:** Although the ultimate goal of classification models is to obtain a reduced detection error rate, different misclassification errors may have different impact on mobile operators, being essential to assign variable costs to different errors.
- **Data Imbalance:** Since cellular network's severe degradation are infrequent events, the collected training data tend to be significantly imbalanced. As a result, the

minority class tends to be misclassified more often than the majority class.

Regarding the implementation of supervised learning models, only Boosting classification algorithms were tested, since these models present a greater performance for several use cases when compared not only to other ML classification algorithms, but also to DNN for tabular data. Thereby, the Boosting classification models tested throughout this work were the following: AdaBoost, Gradient Boosting, XGBoost, Catboost and LightGBM.

Regarding the performance evaluation metric it was required to choose a technique that took into account the non-balancing between classes. To address this issue, the F1-score metric was selected, as suggested by [6]. This function is given by the harmonic mean of precision and recall:

$$F1score = 2 \times \frac{Precision \times Recall}{Precision + Recall} \quad (2)$$

reaching its best value at 1 and worst score at 0.

Lastly, the Stratified 10-Fold Cross-Validation technique was implemented, in order to evaluate the model's generalization performance, by detecting overfitted models. This technique has the particularity of ensuring that when splitting the dataset, the class distribution in each subset matches the class distribution in the total training set, avoiding the existence of folds with few or no data belonging to the minority class [7].

D. Shapley Additive Explanations

In this final phase, the SHAP method is applied to interpret the outputs of the selected models by computing the contribution of each input feature in the produced predictions. This method calculates the Shapley values given by the average of all features contributions, considering all possible coalitions. The Shapley values are represented as an additive feature attribution method. In this work, it was used a variant of SHAP for tree-based ML models, designated TreeSHAP [8] [9].

III. FAILURES DETECTION

After proceeding with the data pre-processing and feature selection phases, the number of input features was reduced to 223 PM counters. Hereupon, the binary failure labelling process and the ML classification models mentioned in Section II were implemented. Table I summarizes the obtained results for the five boosting classification models applied to the User DL Average Throughput KPI.

TABLE I
OBTAINED RESULTS FOR THE CLASSIFICATION BOOSTING ALGORITHMS.

KPI	Failure threshold	Binary labelling	Model	F1 score	10-Fold cross validation
User Downlink Average Throughput (Mbps)	< 7 Mbps	0 : 26789 samples	AdaBoost	0.849	0.823
			GradientBoosting	0.863	0.838
		1 : 7480 samples	XGBoost	0.867	0.849
			CatBoost	0.852	0.838
			LightGBM	0.877	0.853

Finally, the TreeSHAP method was implemented. This SHAP method variant is used since the decision-tree-based ensemble LightGBM algorithm was the best performing model, achieving a maximum F1-score of 0.87. Table II illustrates the obtained confusion matrix.

TABLE II
CONFUSION MATRIX OBTAINED FOR USER DL AVERAGE THROUGHPUT.

		Predicted Label		Total
		0 (Non failure)	1 (Failure)	
True Label	0 (Non failure)	6448	226	6674
	1 (Failure)	237	1657	1894
Total		6685	1883	8568

In turn, Fig. 1 illustrates the respective SHAP Summary Plot, which provides a high-level analysis for each feature importance, sorted in descending order.

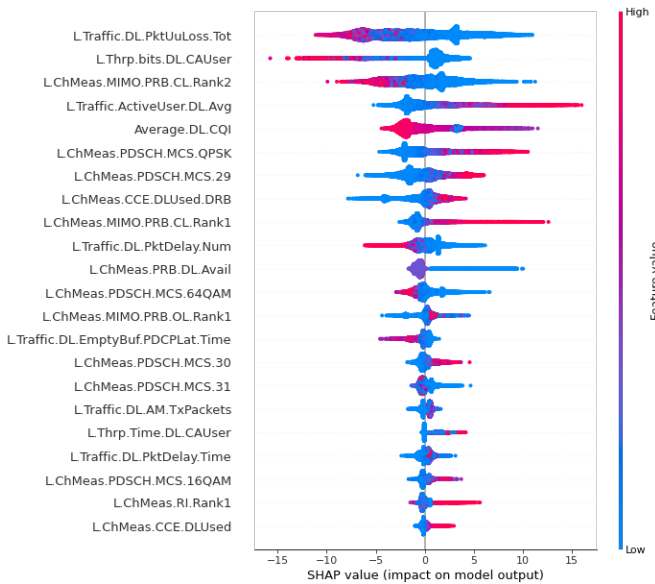


Fig. 1. SHAP summary plot for User DL Average Throughput prediction.

While the x-axis represents the Shapley values, in which the positive values are indicative of *label 1* and the negative values of *label 0*, the y-axis represents each feature. In turn, the color illustrates the feature's values, with the highest ones being represented in pink and the lowest ones in blue. For example, analyzing the L.ChMeas.CCE.DLUsed counter, it is verified that higher values of this feature contribute to the attribution of *label 1*. That is, the pink samples of this feature are mostly on the positive x-axis. On the other hand, lower values contribute to the attribution of *label 0*, since the blue samples are mostly distributed in the negative x-axis. This happens since the Physical Downlink Control Channel (PDCCH) uses aggregation layers in groups of 1, 2, 4 or 8 Control Channel Elements (CCEs), based on radio conditions. Thus, while a User Equipment (UE) in good radio condition requires 1 CCE, a UE in poor radio coverage may require 8 CCEs.

IV. FAILURES DIAGNOSIS

Diagnosing the causes of low throughput is a complex process that requires in-depth knowledge of the network operation, being often a time-consuming task for the network engineers. Thus, the following analysis aims to identify three main causes of throughput degradation, listed in Table III, from the analysis of the obtained SHAP Summary Plot.

TABLE III
MAIN CAUSES FOR THROUGHPUT DEGRADATION.

Failures	Typical causes
Configuration problems	Misadjusted configuration parameters
Radio link problems	Lack of coverage or high interference
Capacity problems	Low capacity in traffic and control channels

The User DL Average Throughput specifies the average DL throughput assigned to each UE in a cell. Thereby, increasing the L.Traffic.ActiveUser.DL.Avg counter, given by the average number of activated UEs in DL, leads to a decrease in the DL throughput, since the resource usage is shared within the available bandwidth, as illustrated by the SHAP dependence plot of Fig. 2.

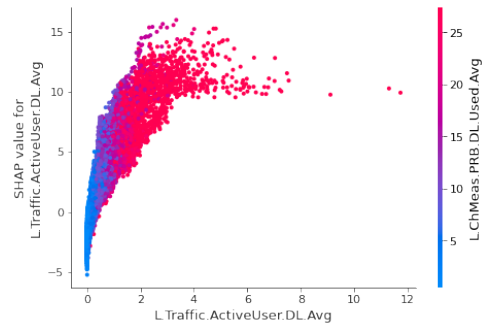


Fig. 2. SHAP dependence plot between the L.Traffic.ActiveUser.DL.Avg and L.ChMeas.PR.B.DL.Used.Avg counters.

Fig. 2 shows that when the average number of activated UEs in DL increases, the L.ChMeas.PR.B.DL.Used.Avg counter, given by the average number of used Physical Downlink Shared Channel (PDSCH) Physical Resource Blocks (PRBs) in DL, also increases, contributing to User DL Average Throughput degradation, since these points are mostly distributed on the positive SHAP values axis. In this situation, so that each user's experience is not affected, it may be necessary to increase the Inactivity Timer, which controls the transition from RRC_CONNECTED to RRC_IDLE state. Thereby, an UE is connected if it has at least one established Dedicated Radio Bearer (DRB). Once there is no more traffic in the transmit buffer, the UE continues in the RRC_CONNECTED state for a defined period of time. If in this period of time it does not detect any traffic, the UE switches to the RRC_IDLE state. Thus, by decreasing the value of the Inactivity Timer parameter, it is possible to support more UEs in the connected state, which can lead to network congestion. On the other hand, by increasing the value of this parameter, it is possible

to improve the overall throughput. However, if this parameter assumes very high values, it is also possible that some UEs use more resources than necessary. Thus, this parameter must be optimized by balancing these two situations. Therefore, engineers' first approach to solving low-throughput problems caused by a high number of users should be to adjust the Inactivity Timer configuration parameter.

Still regarding Fig. 2, it is possible to verify the existence of some pink dots, that is, a high average number of used PDSCH PRBs, for low `L.Traffic.ActiveUser.DL.Avg` values, corresponding to a degradation of the User DL Average Throughput KPI. This situation corresponds to a problem of low network capacity, in which the number of available PRBs for DL is not enough to meet throughput requirements.

Continuing to analyse Fig. 1, it is possible to verify that when the `L.ChMeas.PDSCH.MCS.QPSK` counter, which measures the number of times that Quadrature Phase Shift Keying (QPSK) Modulation and Coding Scheme (MCS) indexes are scheduled on the PDSCHs, increases, the model detects more failures in User DL Average Throughput. On the other hand, when the `L.ChMeas.PDSCH.MCS.64QAM` counter, which measures the number of times that 64-Quadrature Amplitude Modulation (QAM) MCS indexes are scheduled on the PDSCHs, increases, the model detects fewer low throughput situations. Although most of the times, these counters indicate radio problems as the cause of severe throughput degradation, in a first analysis, the problem resolution must be initialized by trying to adjust Channel Quality Indicator (CQI) reports configuration parameters, as will be explained below. The deterioration of the channel's radio conditions, either due to lack of coverage or due to high interference, is identified by a low Signal-to-Interference-plus-Noise Ratio (SINR) value, measured by the UE. This value is converted into a lower CQI to the E-UTRAN NodeB (eNB), which results into a lower MCS index, as illustrated by the SHAP dependence plot of Fig. 3.

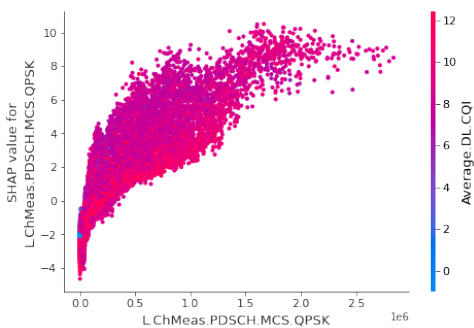


Fig. 3. SHAP dependence plot between the `L.ChMeas.PDSCH.MCS.QPSK` and `Average.DL.CQI` counters.

However, this decrease in throughput may not correspond to a permanent scenario since some vendors use conservative CQI selection algorithms. Therefore, the eNB may use a most conservative CQI value during some transmissions, while continuously monitoring the Block Error Rate (BLER) value.

If after some transmissions the CQI value is maintained, the eNB converges its value to the one initially reported by the UE. The convergence of the CQI and MCS to their actual values results in increased DL throughput. Additionally, the configuration of the CQI reports periodicity must be verified, in order to ensure that it is adapted to the characteristics of each UE. If these solutions do not allow to increase the User DL Average Throughput, the next approach is to try to identify a radio link problem. In this case, some possible solutions to overcome these failures are to optimize the antennas' tilts and azimuths or increase the inter-site distance. This failure resolution strategy should also be followed for low throughput situations identified by an increased value of the `L.ChMeas.PDSCH.MCS.29` counter, or a reduced value of the `L.ChMeas.PDSCH.MCS.31` counter, which indicate the number of times that MCS is changed to QPSK and 64-QAM, respectively, during re-transmissions.

In turn, the `L.ChMeas.MIMO.PR.B.CL.Rank1` and `L.ChMeas.MIMO.PR.B.CL.Rank2` counters, which measure the number of used DL PRBs in closed-loop Rank 1 and 2, respectively, have a leading role in detecting throughput degradation. Namely, while an increased number of Rank 1 reports favors the detection of throughput failures, an increased value of Rank 2 reports is associated with higher DL throughput. Thereby, the Rank Indicator (RI) value gives information about the antenna layer reception, being only reported if the UE is in Multiple Input Multiple Output (MIMO) mode. While for Rank 1 a single antenna signal is transmitted, for Rank 2 spatial multiplexing is used. Thus, when the number of Rank 1 reports increases, radio engineers must first ensure that the switching system between transmission modes is correctly configured and that each UE has access to the highest possible throughput. If once again it is not possible to solve the throughput degradation by re-configuring network parameters, the radio channel degradation troubleshooting already presented should be tested.

Lastly, analysing once again Fig. 1, it is verified that the `L.ChMeas.CCE.DLUsed.DRB` and `L.ChMeas.CCE.DLUsed` counters, related with the number of used CCEs per PDCCH, are critical features for the model decision making. As explained above, a increased number of PDCCH resources usage leads to a reduced number of available resources for the PDSCH, which implies a decrease in DL throughput. In this way, these counters may alert radio engineers to situations of low DL throughput caused by radio link problems or high PDCCH capacity consumption. A possible solution that can be implemented to the last problem is the addition of new cells.

Once defined the most critical PM counters to detect failures in the User DL Average Throughput KPI, and taking into account the work developed in [10], as well as the documentation in [11], the flowchart of Fig.4 was created to determine the most probable DL throughput degradation cause for each site. Thus, this flowchart aims to categorize the 7480 DL throughput failures, measured in the 19 sites, in configuration, radio and capacity problems.

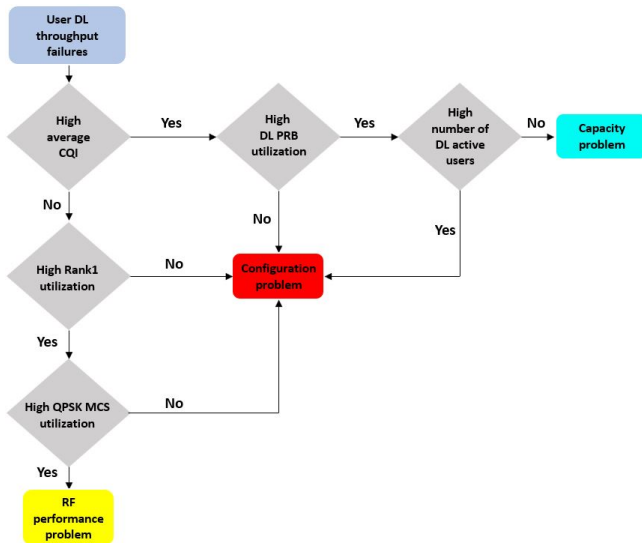


Fig. 4. RCA flowchart for User DL Average Throughput failures.

Fig. 5 not only illustrates the number of failures per site, but also their most likely causes. It was also possible to verify that the failures due to misadjusted configuration are the most frequent, being responsible for 78.12% of the total failures, while radio link and capacity problems are responsible for 17.16% and 4.72%, respectively. This method also allowed the identification of areas of high interference between cells.

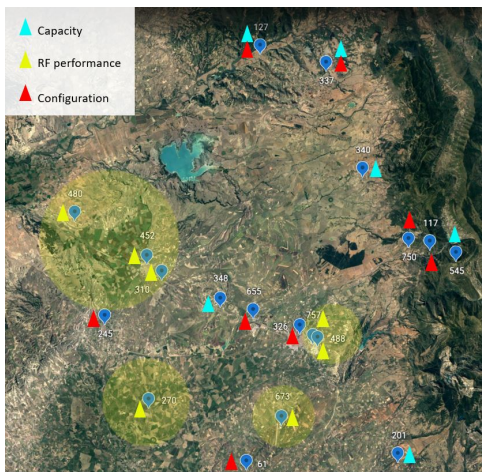


Fig. 5. Distribution of the most likely causes of DL throughput failures across the 19 sites.

V. CONCLUSIONS

The main objective of this work was to detect and diagnose User DL Average Throughput KPI degradation. For this purpose, "Boosting" algorithms and the TreeSHAP method were used to identify the three most recurrent causes of low DL throughput in LTE technology: misadjusted configuration parameters, radio link problems and network capacity limitation, as reported by Network Operations Center's engineers. To this end, the most critical counters to detect failures in each of these categories were identified. Based on these counters, a

failure categorization system was created to diagnose problems in 19 sites. Thus, it was concluded that misadjusted configuration was responsible for 78.12% of the total failures, while 17.16% and 4.72% occurred due to radio link and capacity problems.

Regarding future research, the readjustment of Configuration Management (CM) parameters, based on the failure predictions made by the model, could be tested. In addition, Fault Management (FM) data could be added to the PM counters in order to not only improve the diagnosing performance, but also to determine its accuracy, since the scarcity of diagnostic records for live operation network problems is one of the main limitations in training ML models capable of assisting in RCA. Furthermore, it is intended to extend this diagnostic system to other categories of failures. Lastly, the implementation of this methodology to PM data from 5G networks will be of utmost interest in the near future.

ACKNOWLEDGMENT

This work was carried out in the scope of the international project Cognitive and Automated Network Operations for Present and Beyond (CANOPY) AI2021-061, under the CELTIC-NEXT Core Group and the EUREKA Clusters program. The authors would like to thank the COMPETE/FEDER program for funding the national component of the project (14/SI/2021), as well as the Instituto de Telecomunicações (IT) and CELFINET for its support.

REFERENCES

- [1] A. Asghar, H. Farooq, and A. Imran, "Self-healing in emerging cellular networks: Review, challenges, and research directions," *IEEE Communications Surveys and Tutorials*, vol. 20, no. 3, pp. 1682–1709, 2018.
- [2] D. Mulvey, C. H. Foh, M. A. Imran, and R. Tafazolli, "Cell fault management using machine learning techniques," *IEEE Access*, pp. 124514–124539, 2019.
- [3] M. M. Mampaka and M. Sumbwanyambc, "Poor Data Throughput Root Cause Analysis in Mobile Networks using Deep Neural Network," 2019 IEEE 2nd Wireless Africa Conference (WAC), Pretoria, South Africa, 2019, pp. 1-6.
- [4] Huawei, "User Downlink Average Throughput," pp. 1–13, 2020.
- [5] T. Zhang, K. Zhu, and E. Hossain, "Data-driven machine learning techniques for self-healing in cellular wireless networks: Challenges and solutions," pp. 1–7, 2019.
- [6] L. A. Jeni, J. F. Cohn, and F. De La Torre, "Facing imbalanced data—recommendations for the use of performance metrics," in *Affective Computing and Intelligent Interaction (ACII)*, 2013, pp. 245–251.
- [7] F. Pedregosa, G. Varoquaux, A. Gramfort, V. Michel, B. Thirion, O. Grisel, M. Blondel, P. Prettenhofer, R. Weiss, V. Dubourg, J. Vanderplas, A. Passos, D. Cournapeau, M. Brucher, M. Perrot, and E. Duchesnay, "Scikit-learn: Machine learning in Python," *Journal of Machine Learning Research*, vol. 12, pp. 2825–2830, 2011.
- [8] S. M. Lundberg, G. Erion, H. Chen, A. DeGrave, J. M. Prutkin, B. Nair, R. Katz, J. Himmelfarb, N. Bansal, and S.-I. Lee, "From local explanations to global understanding with explainable AI for trees," *Nature Machine Intelligence*, vol. 2, no. 1, pp. 56–67, 2020.
- [9] C. Monar, 2021. 9.6 SHAP (SHapley Additive exPlanations) Interpretable Machine Learning. [Online] Available at: <https://christophm.github.io/interpretable-ml-book/shap.html>. Last Accessed on 27/09/2021.
- [10] D. Parracho, D. Duarte, I. Pinto and P. Vieira, "An Improved Capacity Model based on Radio Measurements for a 4G and beyond Wireless Network", 2018 21st International Symposium on Wireless Personal Multimedia Communications (WPMC), pp. 314-318, 2018.
- [11] Huawei, "eRAN Capacity Monitoring Guide", HUAWEI TECHNOLOGIES CO., LTD., 2016.